scientific reports

OPEN

Preclinical evaluation of a novel antibody–drug conjugate OBI-992 for Cancer therapy

Ting-Yu Chang, Chun-Jung Lin, Shih-Ni Wen, Yi-Chen Wu, Cheng-Yen Wei, Jye-Yu Huang, Yu-Hsuan Tsao, Yu-Jung Chen, Wei-Chien Tang, Yuen-Chin Wu, Wei-Han Lee, Teng-Yi Huang, Tzer-Min Kuo, Wan-Fen Li & Ming-Tain Lai[✉]

Trophoblast cell surface antigen 2 (TROP2), a transmembrane glycoprotein highly expressed in a variety of epithelial cancers, has been considered as a primary therapeutic target for the development of antibody–drug conjugates (ADCs). OBI-992, an investigational TROP2-targeted ADC, is composed of a novel TROP2 antibody (R4702) conjugated to the topoisomerase I (TOP1) inhibitor exatecan through a hydrophilic enzyme-cleavable linker. This study aimed to characterize R4702 and OBI-992 in vitro. TROP2-targeted antibodies sacituzumab and datopotamab were employed as the comparators for R4702. ADCs sacituzumab govitecan (SG) and datopotamab deruxtecan (Dato-DXd) were used as benchmarks for OBI-992. Results revealed that R4702 binds to an epitope that is distinct from sacituzumab and datopotamab. The cytotoxicity of the OBI-992, SG, and Dato-DXd against different cancer cells is comparable despite they have different internalization profile. Upregulation of breast cancer resistance protein (BCRP) was observed in SG-resistant and Dato-DXd-resistant cells, but not in OBI-992-resistant cells. In addition, significant downregulation of TROP2 expression was detected with Dato-DXd-resistant cells and only slightly downregulation with SG- and OBI-992-resistant cells was observed. Moreover, substantial enhancement of cytotoxicity and DNA damage was found in the combination of OBI-992 with a poly (ADP-ribose) polymerase (PARP) inhibitor (talazoparib). Taken together, the findings in this study support further clinical development of OBI-992.

Antibody–drug conjugates (ADCs) are a prominent class of pharmaceuticals currently under intense pursuit for use as a targeted cancer therapy. ADCs are composed of a monoclonal antibody (mAb) that targets a specific antigen on cancer cells and a highly toxic payload that is conjugated to the mAb through a cleavable or non-cleavable linker[1,2]. Upon binding to the target on cancer cells, the ADC is internalized and trafficked to lysosomes to be processed and release its payload, leading to cancer cell death. Since the first ADC was approved by the U.S. Food and Drug Administration (FDA) in 2000, 12 ADCs have been approved worldwide. Hundreds of clinical trials are currently ongoing, and many more are in the preclinical phase, underscoring the therapeutic promise of the ADC approach[3,4].

Trophoblast cell surface antigen 2 (TROP2), also known as tumor-associated calcium signal transducer 2 (TACSTD2), is a transmembrane glycoprotein that belongs to the tumor-associated calcium signal transducer family[5]. It is highly expressed in various human cancers, such as breast, prostate, ovarian, and colorectal cancers[6]. In addition, the expression level of TROP2 positively correlates with poor prognosis in clinical studies and aggressive behavior of cancer cells[5,7,8]. TROP2 has been shown to activate several signaling pathways involved in cancer progression, including MAPK/ERK pathways[9,10]. Moreover, TROP2 can influence the expression of genes associated with cell cycle regulation, apoptosis, invasion, and metastasis[10,11]. As a result, TROP2 has been identified as a promising target for developing anti-cancer therapeutics, with the TROP2-targeted ADC sacituzumab govitecan (SG) approved by the FDA in 2020, followed by datopotamab deruxtecan (Dato-DXd) in 2025, while MK-2870 is currently in late stages of clinical development.

Topoisomerase I (TOP1) plays a critical role in mammals in maintaining genomic integrity by resolving DNA topological stresses and relaxing supercoiled DNA, which is crucial for cellular processes like chromatin replication, transcription, and repair[11,12]. When TOP1 binds to supercoiled DNA, a tyrosine residue (Tyr723) of TOP1 causes a single-strand DNA (ssDNA) break to initiate a relaxation process for subsequent transcription or

OBI Pharma, Inc., 6F, No. 508, Section 7 Zhongxiao East Road, Nangang District, Taipei, Taiwan. ✉email: mingtainlai@obipharma.com

replication[13]. Given the crucial role of TOP1 in genome stability, the FDA has approved several chemotherapeutic TOP1 inhibitors including the camptothecin (CPT) analogs irinotecan and topotecan. CPT and its derivatives bind at the interface of cleaved DNA and TOP1, resulting in the stabilization of TOP1-DNA cleavage complexes (TOP1cc), which prevent TOP1-mediated DNA relaxation, cause DNA damage, and ultimately lead to cell death[14-16]. DNA damage occurs as both persistent ssDNA breaks caused by inhibitor-stabilized TOP1cc and double-strand breaks that arise when ssDNA breaks encounter chromatin replication complexes or transcription machinery[17]. Therefore, CPT and its derivatives function as topoisomerase poisons, trapping the DNA relaxation process at the TOP1cc stage.

CPT derivatives are the major class of TOP1 inhibitors employed as payloads for the development of TROP2 ADCs. SG is a TROP2 antibody that is conjugated with SN-38, a CPT-derived TOP1 inhibitor, through a hydrolyzable linker CL2A[18]. In addition, the TROP2 ADCs Dato-DXd and MK-2870 employ CPT derivatives as payloads (deruxtecan [DXd] and a belotecan derivative, respectively)[19,20]. Exatecan is also a CPT derivative and has been investigated in a phase 3 clinical trial in combination with gemcitabine for pancreatic cancer treatment[21]. Compared to DXd and SN-38, exatecan exhibits better activity in TOP1 inhibition and tumor suppression[22-24]. In addition, exatecan is not a substrate of ATP-binding cassette (ABC) transporters P-glycoprotein (P-gp) and a poor substrate of breast cancer resistance protein (BCRP)[25,26]. Given both P-gp and BCRP play an important role in mediating multi-drug resistance, compounds less sensitive to upregulation of P-gp and BCRP may provide potential advantages in overcoming drug resistance.

The poly (ADP-ribose) polymerase (PARP) family plays a crucial role in detecting various DNA lesions, including those caused by TOP1 inhibitors[24,27,28]. PARP mitigates the toxicity of TOP1cc through its PARylated catalytic activity[24,27,29,30] and promotes replication fork reversal to facilitate potential re-ligation of TOP1cc[31]. PARP inhibitors have been reported to sensitize cells to topoisomerase inhibitors[30,32-35]. Therefore, treatment with the combination of a TOP1 inhibitor-containing ADC and a PARP inhibitor may represent a promising strategy in optimizing cancer treatment and is currently under investigation in clinical settings[36].

OBI-992 is an investigational ADC composed of a novel TROP2 antibody (R4702) conjugated with exatecan through a hydrophilic enzyme-cleavable peptide linker (the structure was revealed in previous manuscript[37]) at a drug-antibody ratio (DAR) of 4. This study presents in vitro characterizations of R4702 and OBI-992. The TROP2 epitope and binding affinity of R4702 were investigated and compared to those of datopotamab and sacituzumab. In addition, OBI-992 was assessed for cytotoxicity in 2D and 3D cancer cell models. Cancer cells resistant to OBI-992, Dato-DXd, and SG were established and analyzed for TROP2, BCRP, and P-gp expression. Finally, the combination of OBI-992 with a PARP inhibitor was investigated for potential synergistic effects based in vitro cytotoxicity assays.

Results

R4702 binds TROP2 at an epitope distinct from that of sacituzumab and datopotamab with high affinity

To determine the binding epitope of the TROP2-targeted antibody R4702, ELISA assays were performed. The affinity of R4702 binding to peptide fragments derived from the cysteine-rich domain (CRD), the thyroglobulin type domain (TY), and the cysteine-poor domain (CPD) of the TROP2 extracellular domain (ECD) were evaluated. The recombinant TROP2 extracellular domain (rECD) served as a positive control. R4702 showed robust binding to rECD and CRD but not TY or CPD fragments, indicating that R4702 specifically binds to the CRD region (Fig. 1A). To further identify the specific binding epitope of R4702, five overlapping CRD peptide fragments were designed and synthesized (Fig. 1B). A robust ELISA signal was observed with the CRD2.1 peptide fragment, but not with the neighboring peptide fragments CRD1.2 and CRD3.1 (Fig. 1B), the binding region was indicated in violet color (Fig. 1C).

To confirm R4702 has a different binding epitope than that of sacituzumab and datopotamab which is known to bind to cysteine-poor domain (CPD), a competitive cell-binding assay was performed. TROP2-expressing pancreatic cancer cells (BxPC3) were pre-treated with unlabeled TROP2 antibodies R4702, sacituzumab, or datopotamab, followed by incubation with a fluorescein-labeled TROP2 antibody (Fig. 1D-F). Compared with samples pre-treated with controls (Herceptin or no antibody), low levels of fluorescence from fluorescein-sacituzumab or fluorescein-datopotamab were detected on cells in samples pre-treated with unlabeled sacituzumab or datopotamab, respectively. (Fig. 1D, E). This result suggests that datopotamab and sacituzumab recognize epitopes in proximity to each other, interfering with the binding of fluorescein-labeled antibody to the TROP2 protein due to an overlap in binding epitope. In contrast, high levels of fluorescence from fluorescein-sacituzumab or fluorescein-datopotamab were observed on cells in the samples pre-treated with R4702, suggesting R4702 has a different binding epitope from that of sacituzumab and datopotamab. As a result, no substantial reduction of fluorescence signal was observed from fluorescein-R4702 on the cells in samples pre-treated with datopotamab or sacituzumab (Fig. 1F).

Surface plasmon resonance (SPR) was employed to evaluate and compare the in vitro binding affinity of R4702, datopotamab, and sacituzumab to TROP2 protein. R4702 exhibited a relatively higher association rate (Ka: 7.45E + 05/Ms) and lower disassociation rate (Kd: 1.50E-04/s) with TROP2 than datopotamab (Ka: 6.35E + 04/Ms; Kd: 4.09E-03/s) and sacituzumab (Ka: 1.58E + 05/Ms; Kd: 2.65E-04/s) (Fig. 1G). The equilibrium dissociation constant (KD) values showed that R4702 (2.01E-10 M) had TROP2 binding affinity 320- and 8-fold higher than datopotamab (6.43E-08 M) and sacituzumab (1.67E-09 M), respectively. The substantially higher affinity of R4702 compared to datopotamab may be attributed to faster on-rate and slower off-rate R4702 binding to TROP2 (Fig. 1G).
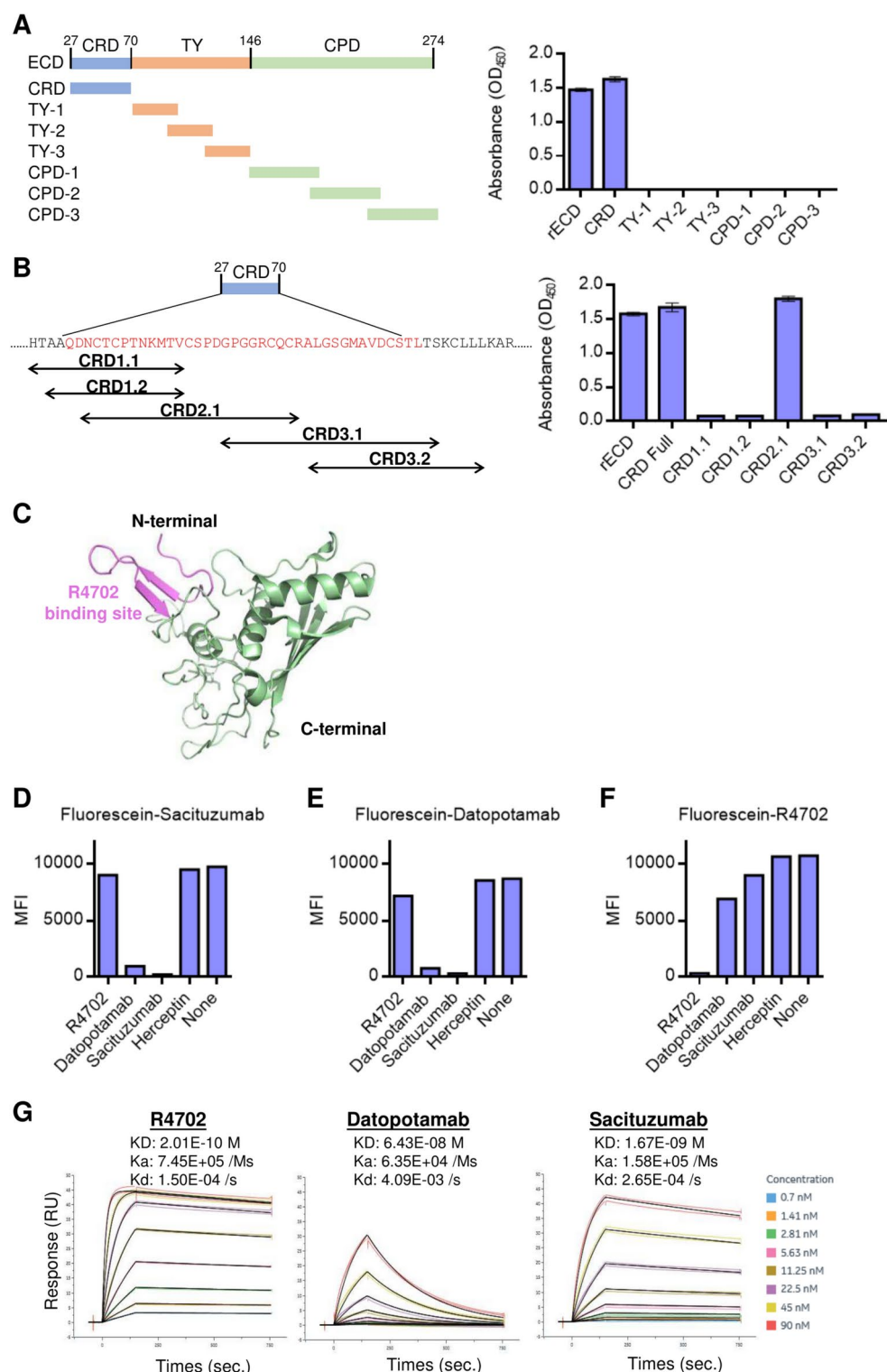
Fig. 1. Investigation of the R4702 binding epitope and binding affinity to TROP2 protein and TROP-2 expressing cells. (A) Evaluation of R4702 binding to different fragments of the extracellular domain (ECD) of TROP2. (B) Investigation of the specific binding epitope of R4702 in the ECD. ELISA assays were performed for both (A) and (B) by incubating the indicated peptides with R4702 followed by measuring the absorbances at 450 nM. (C) The antibody binding region in TROP2 structure (PDB 7E5M). According to the epitope mapping, the R4702 antibody binding to the CRD2.1 (sequence 32–57), indicated by violet color. (D-F) Competition binding assays. BxPC3 cells were pre-treated with the antibody indicated in the X-axis followed by incubation with fluorescein-sacituzumab (D), fluorescein-datopotamab (E), or fluorescein-R4702 (F). (G) Monitoring the binding affinity of TROP2 antibodies to TROP2 protein by surface plasmon resonance. Ka, Association rate constant; KD, equilibrium dissociation constant; Kd, dissociation rate. MFI, mean fluorescence intensity.

Binding and internalization of R4702 and OBI-992 are evaluated with TROP2-expressing cancer cells

Flow cytometry was used to evaluate the binding affinity of TROP2 antibodies R4702 to TROP2-expressing cancer cells with datopotamab and sacituzumab as comparators. Although R4702 displayed better TROP2 affinity based on SPR measurements as aforementioned, it exhibited comparable cell binding affinity with datopotamab and sacituzumab in both breast (MCF-7) and gastric (NCI-N87) cancer cells (EC_{50} range: 1.9 nM to 7.8 nM; Fig. 2A).

To trigger cell killing effects, ADCs must be internalized by target cells to release their cytotoxic payloads. Therefore, internalization of R4702 and OBI-992 by TROP2-expressing pancreatic (BxPC-3) and gastric (NCI-N87) cancer cell lines was assessed using a flow cytometry-based assay. The maximum internalization of OBI-992 and R4702 was approximately 40% at 2 h in BxPC-3 cells and 4 h in NCI-N87 cells (Fig. 2B). When compared with benchmark antibodies, the maximum internalization level of R4702 was lower than that of sacituzumab and datopotamab, but higher than the reference anti-HER2 trastuzumab. In addition, the internalization level of ADCs, including R4702 ADC (OBI-992), Datopotamab ADC (Dato-DXd), Sacituzumab ADC (SG), and Herceptin ADC (Enhertu), was assessed and is shown in Fig. 2C. The results showed that the internalization profiles of ADCs were similar to that of parental antibodies (Fig. 2C), suggesting that linker/payload conjugation had no impact on antibody internalization.

OBI-992 cytotoxicity positively correlates with TROP2 expression levels

To compare the potency of ADC TOP1 inhibitors, the cytotoxicity of exatecan, DXd, and SN-38 was evaluated across different cancer cell types (Fig. 3A). Exatecan demonstrated cytotoxicity against triple-negative breast (MDA-MB-231), gastric (NCI-N87), and pancreatic (Capan-1) cancer cells with IC_{50} values of 0.73 nM, 0.95 nM, and 1.04 nM, respectively. The corresponding IC_{50}s values were 2.72 nM, 3.77 nM, and 2.62 nM for DXd and 4.02 nM, 3.37 nM, and 3.60 nM for SN-38, respectively (Fig. 3A). These results indicated that exatecan displayed 2- to 5-fold better potency than DXd and SN-38 against the three different cancer cell lines (Fig. 3A).

To compare the ability of TOP1 inhibitors in inducing DNA damage within cancer cells, Western blot analyses were used to assess levels of DNA damage biomarkers in triple-negative breast cancer cells (MDA-MB-231) treated with either exatecan, DXd, or SN-38 at various concentrations. DNA damage markers included phosphorylation of histone H2A family member X at serine 139 (γH2AX) and replication protein A subunit 2 (RPA2) at serine 4 and 8 (RPA2 pS4/S8). A dose-dependent increase in the signal of DNA damage markers was observed in the presence of each of the TOP1 inhibitors tested (Fig. 3B). The results showed higher levels of RPA2 pS4/S8 and γH2AX in cancer cells treated with 7.5 μM exatecan compared to cells treated with 35 μM DXd and SN-38.

To evaluate the relationship between OBI-992 cytotoxicity and TROP2 expression levels, the IC_{50} of OBI-992 was measured in 9 cancer cell lines with varying levels of TROP2 expression. TROP2 expression levels were determined by quantitative FACS. Results showed a positive correlation between OBI-992 IC_{50} and TROP2 expression, as indicated by Spearman correlation (Fig. 3C; r = -0.8, P = 0.0138); detailed values are shown in Supplementary Table 1. In addition, a 3D spheroid model of prostate cancer (DU-145 cells) was established to emulate tumor-like tissue structure and function. The cellular toxicity of TROP2 ADCs SG, Dato-DXd, and OBI-992 were evaluated in the spheroid model. OBI-992 demonstrated comparable levels of cytotoxic activity at similar concentrations to Dato-DXd, whereas SG exhibited much higher cellular toxicity at lower concentrations (Fig. 3D).

ATP-binding cassette (ABC) transporters BCRP and P-gp were not upregulated in OBI-992-resistant cells

Since ADCs are composed of an antibody linked to a payload, ADC resistance may be attributed to downregulation of the ADC antibody target and/or a high rate of payload removal once the ADC is internalized into the cells, or due to a mutation in payload binding proteins. To investigate mechanisms contributing to TROP2-ADC resistance, DLD-1 colon cancer cell lines with acquired resistance to TROP2-ADCs were established. Cells underwent chronic exposure to either SG, Dato-DXd, or OBI-992 to induce resistant cell lines. Less than 20% reduction in cell viability was observed in ADC-resistant cells when treated with SG, Dato-DXd, and OBI-992 at IC_{50} concentrations (Fig. 4A). Western blot analyses were performed to evaluate the levels of TROP2 protein in SG-resistant (R-SG), Dato-DXd resistant (R-Dato-DXd), and OBI-992-resistant (R-OBI-992) cells. Slightly lower levels of TROP2 protein expression were observed in R-OBI-992 and R-SG cells compared with the expression level in parental cells, whereas substantially lower levels of TROP2 expression were observed in R-Dato-DXd cells versus parental cell controls (Fig. 4B). It is known that both P-gp and BCRP are distinct ABC transporters that transport small molecules outside of cells, thus conferring resistance to various chemotherapy drugs[38]. Therefore, the expression level of both proteins was investigated by Western blot. BCRP levels were higher in both R-SG and R-Dato-DXd cells, with considerably higher levels observed in R-SG compared to R-Dato-DXd samples (Fig. 4B). In contrast, BCRP levels were comparable between R-OBI-992 cells and parental cell controls (Fig. 4B). No differences in P-gp levels were detected among the three resistant cell lines compared to parental cells.

OBI-992 demonstrated synergistic effects in combination with PARP inhibitors

TOP1 inhibitors have been shown to exhibit synergistic effects with poly (ADP-ribose) polymerase (PARP) inhibitors[30,32,39], prompting an evaluation of potential combination effects between PARP inhibitors and OBI-992. A screening study was performed to assess the cytotoxicity of exatecan in combination with four FDA-approved PARP inhibitors— talazoparib, rucaparib, niraparib, and olaparib (Figure S1). A low toxic dose of exatecan (0.4 nM) was employed in different cancer cell lines to assess whether the TOP1 inhibitor can exert
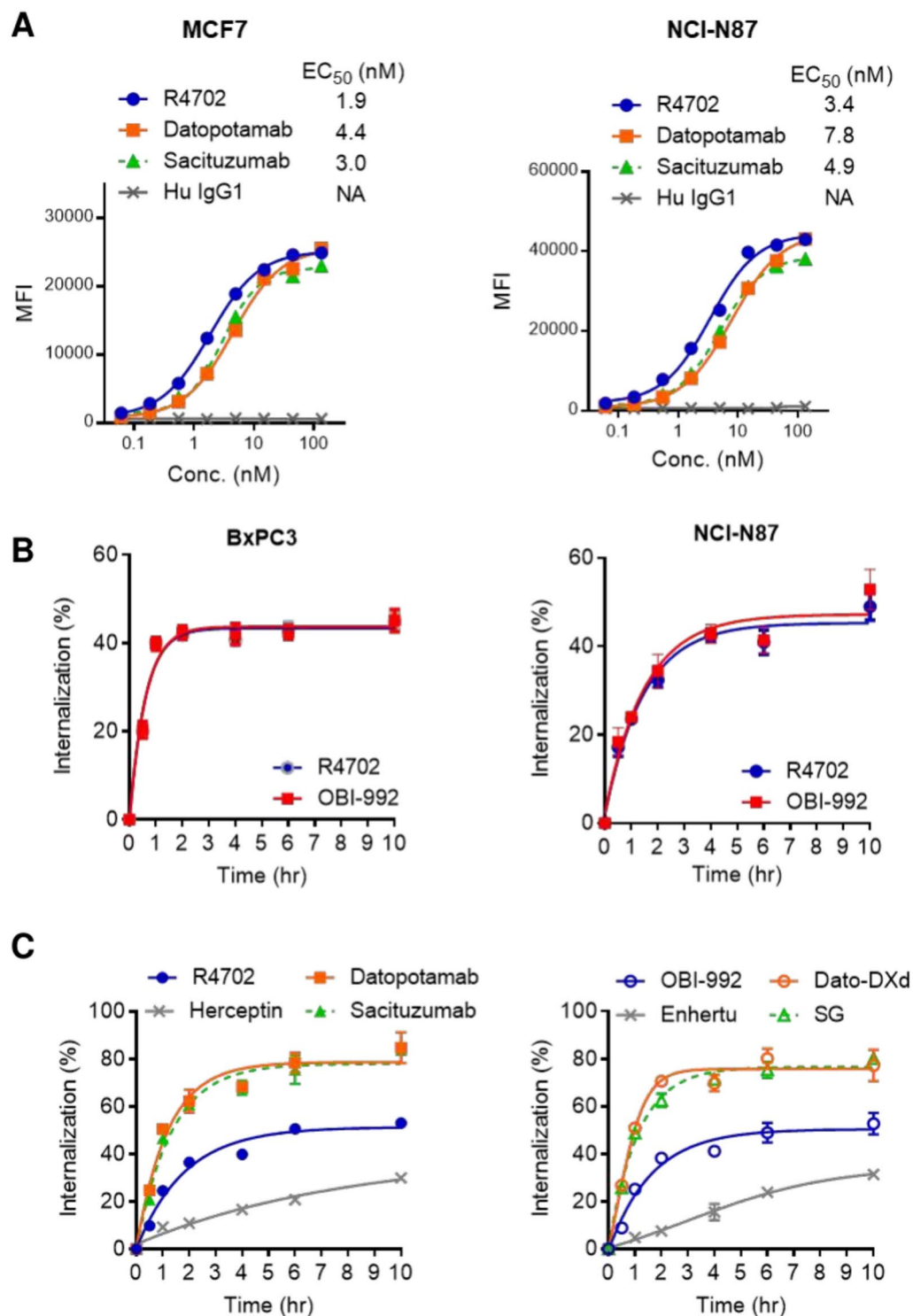
Fig. 2. Internalization profiles of TROP2 antibodies and corresponding ADCs. (**A**) Evaluation of the binding affinity of TROP2 antibodies to TROP2 expressing cells. MCF7 (left panel) and NCI-N87 (right panel) cells were incubated with the indicated TROP2 antibody followed by detection using FITC-conjugated anti human IgG antibody. MFI was quantified by flow cytometry. (**B**) The internalization profile of OBI-992 and its native antibody R4702. BxPC3 (left panel) and NCI-N87 (right panel) cells were treated with fluorescence-labeled OBI-992 or R4702. The internalization kinetics were measured by flow cytometry. (**C**) Internalization kinetic profiles of R4702, OBI-992, and benchmark antibodies and ADCs. The internalization of anti-TROP2 antibodies (left panel) and anti-TROP2 ADCs (right panel) was measured. An anti-HER2 antibody (herceptin) and its ADC Enhertu were included as for references. EC_{50}, half maximal effective concentration; Hu IgG1, human immunoglobulin G1; Dato-DXd, datopotamab deruxtecan; SG: sacituzumab govitecan.
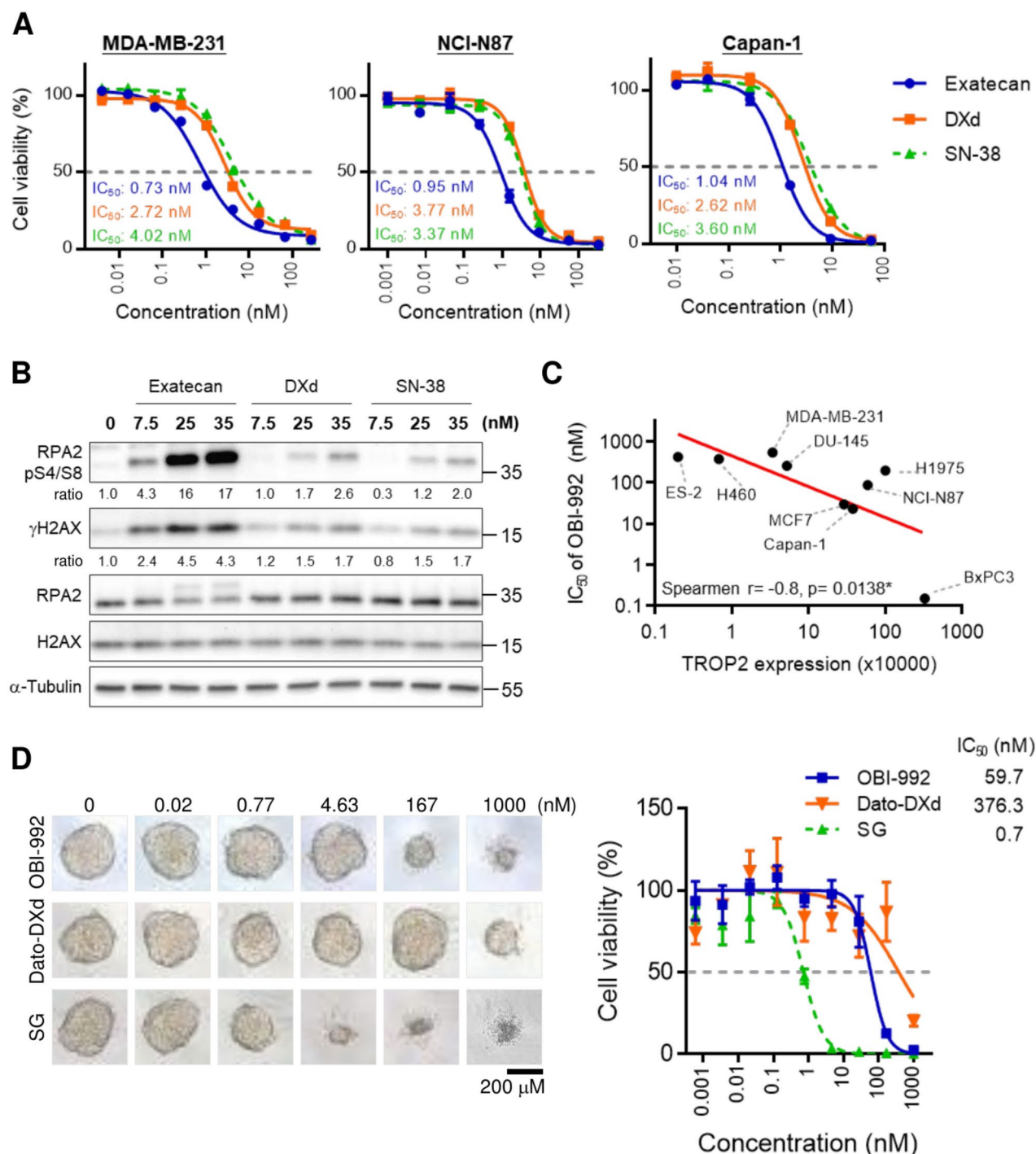
Fig. 3. Evaluation of the potency of topoisomerase 1 (TOP1) inhibitors and TROP2 ADCs in various cancer cells. (**A**) Determination of the cytotoxicity of topoisomerase 1 (TOP1) inhibitors in different cancer cell lines. Data are presented as mean and SD (n = 3). The IC_{50} values of each group were calculated by GraphPad Prism 6 (**B**) Western blot analysis of DNA damage marker RPA2 pS4/S8 and γH2AX in MDA-MB-231 treated with TOP1 inhibitor for 3 h. (**C**) The correlation between TROP2 expression levels in different cancer cell lines and the potency of OBI-992. TROP2 expression was determined by quantitative FACS. Spearman correlation was employed for the analysis. (**D**) Assessment of cell viability of DU145 in 3D spheroid cells treated with TROP2 ADCs. Representative images of the spheroids are shown (left). Percentages of cell viability were calculated, and results are presented as mean and SD (n = 3) (right). Dato-DXd, datopotamab deruxtecan; IC_{50}, half-maximal inhibitory concentration; SG, sacituzumab govitecan; TROP2, trophoblast cell surface antigen 2.
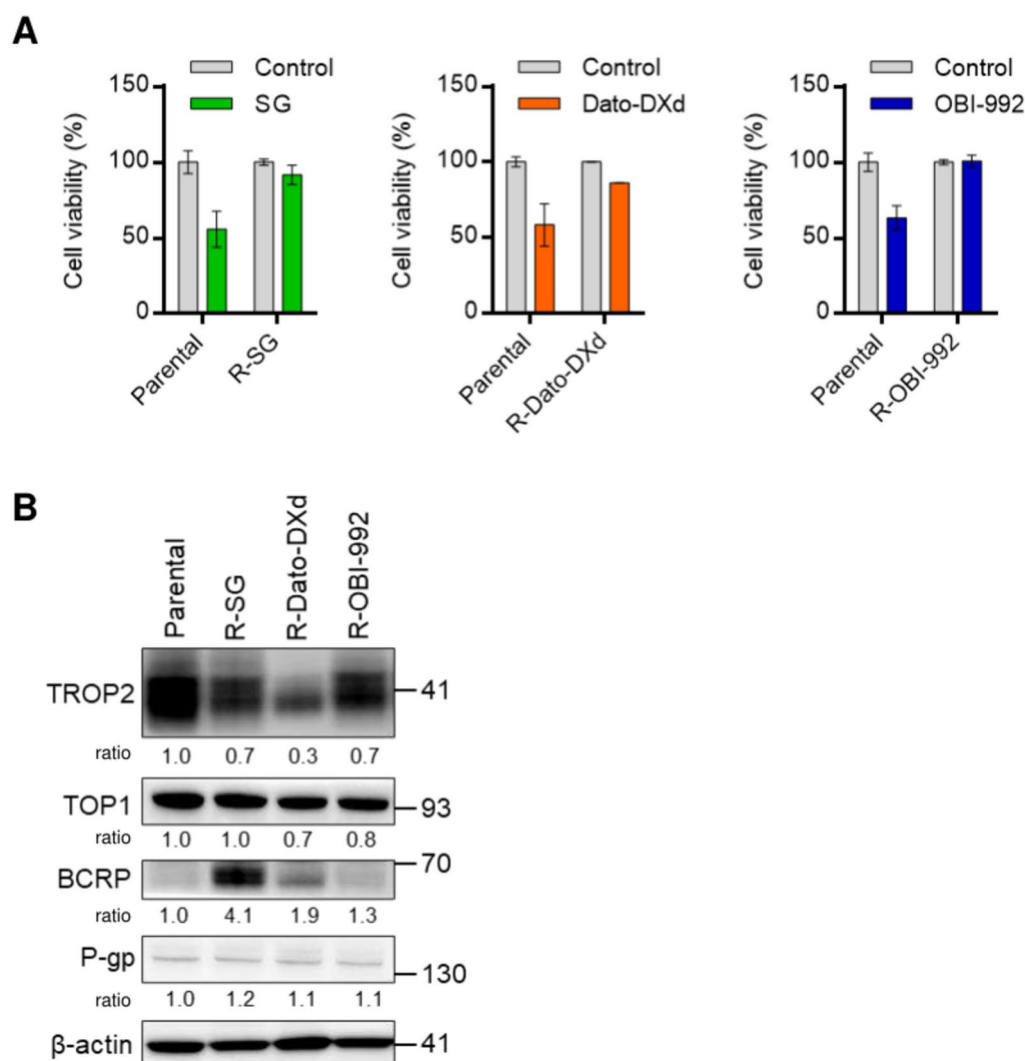
Fig. 4. Characterization of resistant cell lines of TROP2-targeted ADCs. (**A**) Cell viability of parental cells and resistant cells treated with ADCs at the following concentrations: SG: 1 nM; Dato-DXd: 100 nM; OBI-992: 100 nM. (**B**) Evaluation of the impact of TROP2-ADC induced resistance on the expression of TROP2, TOP1, BCRP, and P-gp in the DLD1 cell line via Western blot. BCRP, breast cancer resistance protein; R-Dato-DXd, datopotamab deruxtecan-resistant cells; R-OBI-992, OBI-992-resistant cells; R-SG, sacituzumab govitecan-resistant cells; P-gp, P-glycoprotein; SG, Sacituzumab govitecan; TOP1, topoisomerase 1; TROP2, trophoblast cell surface antigen 2.

synergistic effects in combination with PARP inhibitors; the low dose of exetacan only reduced cell viability by 10–20%. Talazoparib exhibited a 42-fold improvement in IC_{50} values when combined with exatecan in MDA-MB-231 cells, reducing the IC_{50} value from 169 to 4 nM. The other PARP inhibitors (rucaparib, niraparib, and olaparib) showed 2- to 3-fold potency enhancement in the combination study (Figure S1). The same trends were observed in NCI-N87 cells, with cytotoxicity of different PARP inhibitors increased 1.7- to 8.6-fold in the presence of exatecan; talazoparib displayed the strongest potency enhancement with exatecan combination treatment (Figure S1). Similar effects were observed from the combination of PARP inhibitors with DXd or SN-38 (Figure S2).

Given that talazoparib displayed the highest synergistic effects with TOP1 inhibitors, talazoparib was further evaluated in combination with OBI-992. Consistent with above observations, synergistic effects were also observed in different cancer cell lines (MDA-MB-231, NCI-N87, and Capan-1; Fig. 5A). In MDA-MB-231 cells, the IC_{50} value of talazoparib was 32-fold higher than the IC_{50} in the combination study with OBI-992 (338 nM vs 11 nM). In addition, the potency of talazoparib was enhanced 9-fold in NCI-N87 cells (IC_{50}: 297 nM vs 33 nM), and enhanced 4-fold in Capan-1 cells (IC_{50}: 29 nM vs 7 nM) (Fig. 5B).

To investigate the potential mechanism of the synergistic effect, the level of DNA damage in response to combination treatment was evaluated. After 24 h of combined treatment with OBI-992 and talazoparib, levels of the DNA damage marker γH2AX were higher than those observed for OBI-992 or talazaoparib alone (Fig. 5C), suggesting that greater DNA damage occurred in the presence of both TOP1 and PARP1 inhibitors.
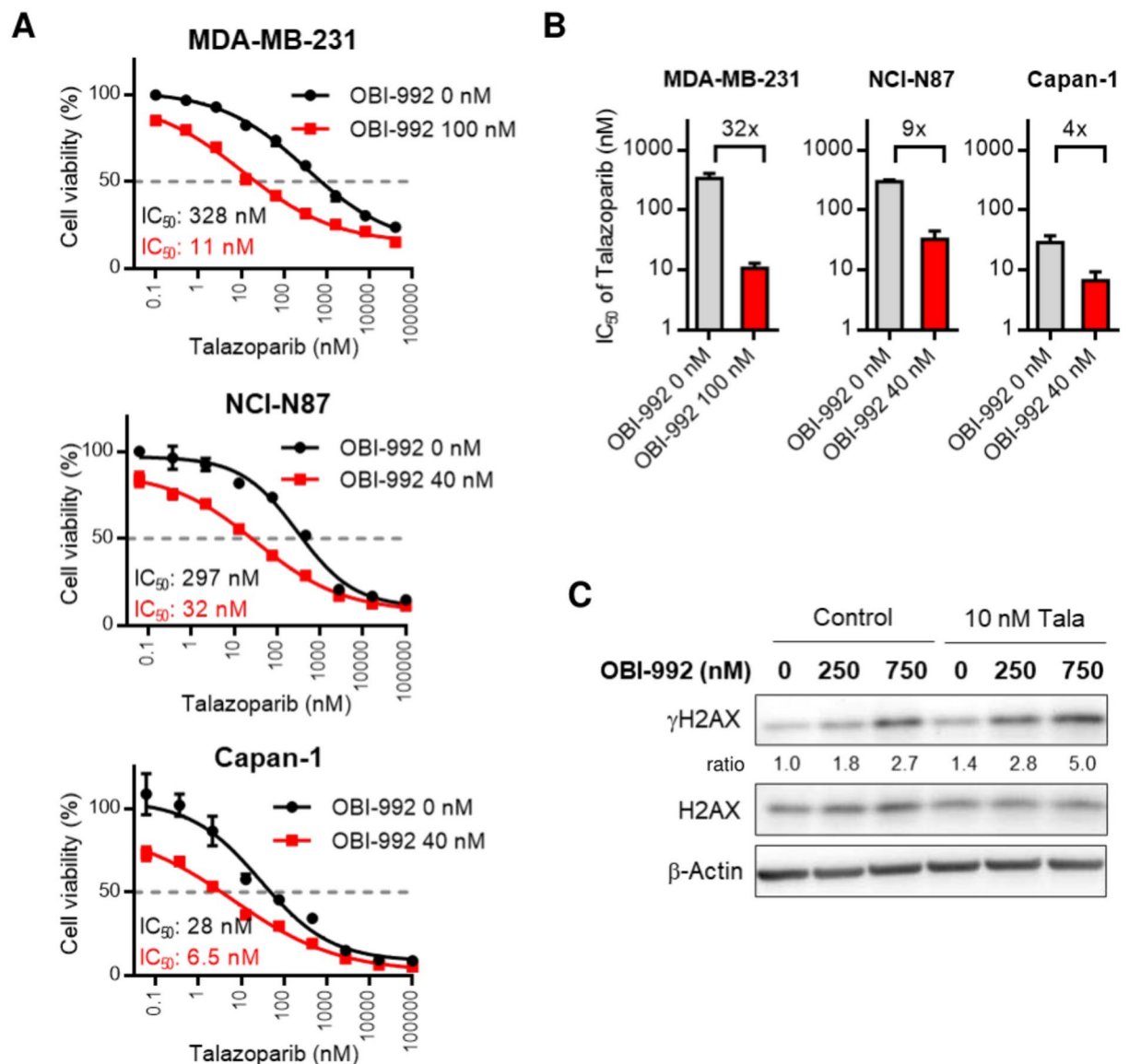
Fig. 5. Evaluation of the synergistic effects of OBI-992 with PARP inhibitor talazoparib. (**A**) Determination of the cytotoxicity of talazoparib in the presence or absence of OBI-992 in different cell lines. Percentages of cell viability were calculated, and results are presented as mean and SD (n = 3). (**B**) Fold change of the IC_{50} of talazoparib in the presence or absence of OBI-992 in the three cell lines. (**C**) Western blot analysis of the DNA damage marker γH2AX in MDA-MB-231 treated with talazoparib and OBI-992 for 24 h. The data in this figure are from separate gel electrophoresis runs with consistent loading of the same samples. γH2AX; histone family member X at serine 139; IC_{50}, half-maximal inhibitory concentration.

Discussion

ADCs have gained significant attention in the field of cancer therapeutics due to their ability to deliver toxic payloads to targeted cancer cells, minimizing potential off-target effects and increasing the therapeutic window of the anticancer drugs. In this study, in vitro characterizations were performed of the investigational ADC, OBI-992, providing insights into distinct attributes of this ADC and its potential for an improved clinical profile relative to existing TROP2 ADCs.

A key feature of OBI-992 is the TROP2 antibody (R4702) used in its design. ELISA binding assays summarized here (Fig. 1) establish that R4702 binds to a distinct epitope on TROP2's CRD that is different from the binding epitopes of sacituzumab and datopotamab, which bind to the cysteine-poor domain (CPD) region of TROP2[40,41]. Further investigation of the specific binding site of R4702 on CRD revealed that R4702 exclusively binds to the region of CRD2.1. Based on sequence comparisons among the neighboring peptide fragments CRD1.2, CRD2.1, and CRD3.1, the 4 unique residues SPDG in the CRD2.1 peptide fragment may play an important role in the interaction of TROP2 with R4702. These results, together with competitive binding

results, indicate that R4702 represents a novel TROP2 antibody. As a result, OBI-992 may have an advantage in overcoming resistance derived from mutations in the binding epitope of sacituzumab and datopotamab.

OBI-992 demonstrated high cytotoxic activity in both 2D and 3D spheroid cultures across various cancer cell types, and a positive correlation between OBI-992 cytotoxicity and TROP2 expression in cancer cells was observed (Fig. 3). Exatecan exhibited greater cytotoxicity and correspondingly greater DNA damage than the other two payloads (DXd and SN-38). Given the higher potency of exatecan compared to SN-38, DAR 4 was designed in OBI-992 compared to DAR 8 of SN-38 in SG to minimize off-target toxicity[39–45].

Understanding the mechanisms leading to TROP2 ADC resistance is crucial for devising effective strategies to overcome it and to optimize the clinical utility of ADCs in development. Mechanisms of resistance may involve the downregulation of, or a mutation in the target proteins and/or alterations in drug transport or efflux mechanisms[46,47]. Specific variants, such as the R364H mutation on TOP1, can lead to alterations of the structure in the binding pocket of topoisomerase 1, rendering it less susceptible to inhibition by the payload[48]. Other mechanisms of resistance involve TROP2 mutations, including the T256R mutation that has been associated with SG resistance due to impaired plasma membrane localization and reduced cell-surface binding of sacituzumab[49]. Further investigation will be needed to determine whether other mutations in TOP1 or TROP2 are associated with OBI-992 resistance. This study evaluated resistance mediated through the ABC transporter proteins BCRP and P-gp, which expel cytotoxic drugs and may therefore be a primary mechanism for the development of multidrug resistance[44]. The overexpression of BCRP has been previously identified as a factor that enhances resistance to TOP1 inhibitors, including SN-38 and topotecan[50]. In our study, upregulation of BCRP was found in R-SG and R-Dato-DXd cells (Fig. 4) but was not observed in R-OBI-992 cells. This is not surprising as exatecan is a weak substrate of BCRP[28]. Furthermore, resistance to Dato-DXd may be also due to the downregulation of TROP2 (Fig. 4). This is of interest as both sacituzumab and datopotamab bind to the same region in the TROP2 protein, and further investigation on the differences between resistance mechanisms for Dato-DXd and SG is warranted. Since expression patterns for TROP2, BCRP and P-gp did not reveal any substantial differences relative to parental cells in OBI-992-resistant cells in this study, showing only a slight decrease in TROP2 expression with no major increase in either BCRP or P-gp protein expression, it is necessary to conduct further investigation on the potential resistance mechanisms of OBI-992.

PARP inhibitors are currently utilized in clinical cancer therapy for patients with BRCA mutations[48,51]. In our findings, BRCA2-deficient Capan-1 cells or the BRCA wild-type (WT) MDA-MB-231 and NCI-N87 cells exhibited increased sensitivity to four PARP inhibitors when combined with OBI-992 or exatecan. This observation aligns with the findings of Cardillo et al., who demonstrated that SG elicited increased synthetic lethality with PARP inhibitors in BRCA1/2 WT cancer cells[43]. When evaluating the combination of OBI-992 and talazoparib specifically, the impact to cell viability was less pronounced in Capan-1 cells than in the other two cell lines (Fig. 5), which may be attributed to the intrinsic high sensitivity of Capan-1 cells to PARP inhibitors due to their BRCA2 mutation. Nevertheless, the consistent enhancement effect observed across cell lines and conditions in our study suggests that OBI-992 in combination with PARP inhibitors may hold potential clinical benefit beyond cases with BRCA mutations, thus expanding its potential clinical application.

In this study, we conducted a detailed in vitro characterization of OBI-992, a novel ADC targeting TROP2 protein in cancer cells, providing an important foundation for future pre-clinical and clinical evaluation of this ADC. Taken together, the results showed that OBI-992 possesses properties distinct from Dato-DXd and SG, supporting the continued clinical study and development of OBI-992.

Materials and methods
Cell lines and compounds
Human prostate cancer DU145 cells (RRID:CVCL_0105) were cultured in Eagle's Minimum Essential Medium (Corning) with 10% fetal bovine serum (FBS) and 1% penicillin/streptomycin (P/S). Human pancreatic cancer Capan-1 cells (RRID:CVCL_0237) were cultured in Iscove's Modified Dulbecco's Medium (IMDM; Gibco) with 20% FBS and 1% P/S. Human ovary cancer ES2 cells were cultured in McCoy's 5A (Gibco) with 5% FBS and 1% P/S. Human breast cancer MCF7 cells (RRID:CVCL_0031) were kindly provided by Prof. Alice L. Yu, cultured in Minimum Essential Medium (Gibco) with 10% FBS, 1% P/S, and 0.01 mg/mL human recombinant insulin. Human lung cancer, H1975 (RRID:CVCL_1511), H460 (RRID:CVCL_0459), NCI-N87 (RRID:CVCL_1603), and human pancreatic cancer BxPC3 cells (RRID:CVCL_XX78) were cultured in Roswell Park Memorial Institute (RPMI) 1640 (Gibco) with 10% FBS and 1% P/S. All above cell lines were cultured in a humidified incubator at 37℃ with 5% CO2. Human breast cancer MDA-MB-231 cells (RRID:CVCL_0062) were cultured in Leibovitz's L-15 medium (Gibco) with 10% FBS and 1% P/S in a humidified incubator at 37℃ without CO2. All cell lines, except for MCF-7 (RRID:CVCL_0031), were purchased from the American Type Culture Collection (ATCC).

Exatecan (Seedchem, Catalog #: 171,335–80-1), DXd (MedChemExpress, Catalog #: 1,599,440–33-1), SN-38 (Acros organic, Catalog #: 86,639–52-3), and talazoparib (AmBeed, Catalog #: 1,207,456–01-6) were purchased from Seedchem, MedChemExpress, Acros Organics, and AmBeed, respectively. Niraparib (Catalog #: 1,038,915–60-4), olaparib (Catalog #: 763,113–22-0), and rucaparib (Catalog #: 283,173–50-2) were purchased from Combi-Blocks. SG was purchased from Gilead Sciences. Dato-DXd was generated as described in[46].

Preparation of TROP2 antibody
The sequences of R4702, datopotamab, and sacituzumab are based on the information from Biosion, Daiichi Sankyo, and Immunomedics, respectively. The DNA sequence encoding R4702, datopotamab, and sacituzumab were optimized for CHO cells and synthesized in vitro by Genewiz. The DNA was then ligated into the pcDNA3.4 expression vector (Thermo Fisher Scientific) using the NEBuilder DNA Assembly kit (New England Biolabs). The expression plasmids were then transfected to ExpiCHO-S cells (Thermo Fisher Scientific) and

Fragment	Peptide sequence
CRD	HTAAQDNCTCPTNKMTVCSPDGPGGRCQCRALGSGMAVDCSTLTSKC
TY-1	LLLKARMSAPKNARTLVRPSEHALVDNDGLYDPDCDPEGRFKARQCNQTS
TY-2	LVDNDGLYDPDCDPEGRFKARQCNQTSVCWCVNSVGVRRTDKGDLSLRCD
CPD-1	ELVRTHHILIDLRHRPTAGAFNHSDLDAELRRLFRERYRLHPKFVAAVHY
CPD-2	LHPKFVAAVHYEQPTIQIELRQNTSQKAAGDVDIGDAAYYFERDIKGESL
CPD-3	YFERDIKGESLFQGRGGLDLRVRGEPLQVERTLIYYLDEIPPKFSMKRLT
CRD1.1	HTAAQDNCTCPTNKMTVC
CRD1.2	AAQDNCTCPTNKMTVC
CRD2.1	NCTCPTNKMTVCSPDGPGGRCQCRA
CRD3.1	PGGRCQCRALGSGMAVDCSTLTSKC
CRD3.2	GSGMAVDCSTLTSKCLLLKA

Table 1. Design sequences of synthetic TROP2 peptide. The fragment peptides of TROP2 sequence were synthesized by GenScript Biotech.

were produced by ExpiFectamine™ CHO Transfection kit (Thermo Fisher Scientific) with high titer protocol. The secreted antibodies were harvested by collecting supernatant before cell viability dropped below 60%. After centrifugation, the supernatant was stored at 4 °C prior to purification. After harvesting the clarified cell culture medium via centrifugation to remove cells, anti-TROP2 antibody was purified by affinity column using HiTrap Protein A column (Cytiva) and eluted fractions were concentrated by a Millipore Amicon Ultra Filter (10 kDa).

Preparation of OBI-992
Anti-TROP2 antibody R4702 (10 mg/ml, 50.0 ml; preparation described in the section of Preparation of TROP2 antibody) in conjugation buffer (50 mM histidine, 20 mM EDTA, pH 7.0) was reduced with TCEP.HCl (2–3 equivalents) for 2–6 h. To this reduced antibody solution, the conjugated molecule maleimide-hydrophilic linker-exatecan (5–6 equivalents) in DMSO was added. After conjugation for 1 h, the ADC buffer was replaced with storage buffer (20 mM sodium acetate, pH 5.0 with 0.1% (w/w) polysorbate 80) via ultrafiltration/diafiltration to remove free linker-payload to give the final ADC. The drug-to-antibody ratio (DAR) value was determined based on the distribution profile of the ADC with different DAR in hydrophobic interaction chromatography (HIC). The average DAR value of OBI-992 ranges from 3.7 to 4.2.

Enzyme-linked immunosorbent assay (ELISA) for antigen binding
Several peptide fragments of TROP2's extracellular cysteine-rich domain (CRD), thyroglobulin type domain (TY), and cysteine-poor domain (CPD) were synthesized according to sequences listed in the Table 1.

TROP2 human recombinant extracellular domain or synthetic peptide (synthesized by GenScript Biotech) was coated onto a 96-well microplate. Following blocking with SuperBlock Blocking Buffer (Thermo, Catalog #: 37,515), the TROP2 antibody was added and incubated for 1 h at room temperature. Subsequently, a secondary antibody, goat anti-human IgG (Fab specific) peroxidase conjugate (Sigma-Aldrich Catalog #: A0293), was added and incubated for an additional 1 h at room temperature. After washing with buffer, peroxidase substrate TMB (3,3',5,5' – tetramethylbenzidine, Sera Care Catalog #: 5120–0083) was added, and the resulting microplate was incubated at room temperature for 7 min to allow color development. Stop solution (1N HCl) was added to stop the reaction, and the absorbance at 450 nm (OD_{450}) was measured using a SpectraMax M2 reader within 10 min.

Competition binding assay
BxPC3 cells were pre-incubated with a saturated concentration of unlabeled TROP2 antibodies (R4702, datopotomab, or sacituzumab at 30 μg/mL) at 4 °C for 30 min. As negative controls, samples were also pre-treated with trastuzumab or no antibody. Following centrifugal washing, the cells were mixed with 3 μg/mL fluorescein-labeled TROP2 antibodies and incubated at 4 °C for an additional 30 min. After the incubation, fluorescent signals were analyzed using flow cytometry. The mean fluorescence intensity (MFI) of fluorescein-labeled TROP2 antibodies represents the binding ability of each TROP2 antibody after pre-incubation with the same or other TROP2 antibody.

TROP2 binding affinity analysis by surface plasmon resonance (SPR)
To determine the binding kinetics of TROP2 antibody to human TROP2 protein (Acro Biosystems, Catalog #: TR2-H5223), surface plasmon resonance (SPR) experiments were performed on a Biacore 8 K instrument (GE Healthcare, Life Sciences). TROP2 antibodies (10 nM) were covalently immobilized on the surface of Protein A sensor chip by using HBS-EP + buffer, pH 7.4 (Cytiva). The reference flow cell was similarly treated with buffer without antibody. A kinetics experiment was performed with twofold serial dilutions of TROP2 protein (0.7, 1.41, 2.81, 5.63, 11.25, 22.5, 45, and 90 nM) in HBS-EP + buffer, pH 7.4. Identical experimental conditions (flow rate of 30 μL/minutes, contact time 150 s and dissociation time 600 s, and regeneration contact time 30 s) were used for each cycle of measurement. Regeneration of the chip was carried out by washing with glycine HCl, pH 1.5. The level of interaction on the sensor chip is represented as a change in response units (RU). The analysis of

association and dissociation rates was performed using BIA evaluation software (GE Healthcare Life Sciences) with Langmuir fit model of 1:1 binding.

Cell surface binding assay

MCF7 and NCI-N87 cells were incubated with TROP2 antibody at 4 °C for 30 min. After incubation and cell washing, bound TROP2 antibody was detected by secondary antibody, FITC goat anti-human IgG (Fc specific) antibody (Sigma, Catalog #: SI-F9512) at 4 °C for 30 min. Stained cells were washed and resuspended in fluorescence-activated cell sorting (FACS) buffer for immediate flow cytometry analysis (BD FACS Canto II). The FITC fluorescence signals were measured and acquired by FACSDiva Software. Cells were gated and analyzed for MFI to represent binding intensity of each sample. The concentration of half maximal efficacy (EC_{50}) was calculated using GraphPad Prism 6.

Internalization assay

The Zenon Human IgG Labeling kit (Thermo, Catalog #: Z25402) was used for Alexa488 labeling. Briefly, 1 μg of antibody or ADC in phosphate-buffered saline was mixed with 5 μL of the Zenon human IgG labeling reagent (Component A) and incubated for 5 min at room temperature. Five μL of the Zenon human IgG labeling reagent (Component B) was added and incubated for an additional 5 min at room temperature.

The cell-based internalization assay was performed as described with modification[52]. In brief, 1×10^5 cells/mL of NCI-N87 or BxPC-3 cells were seeded in a 96-well microplate, and 0.5 μg of Alexa488-labeled antibodies or ADCs were added to the culture. After incubation for 0, 0.5, 1, 2, 4, 6, or 10 h, cells were lifted by incubating with 100 μL of cell dissociation buffer for 10 min at 37 °C. Cells were harvested, and cell pellets were re-suspended in 2% bovine serum albumin in phosphate buffered saline with (quenched) or without (unquenched) anti-Alexa488 IgG for 30 min at 4 °C.

The MFI of the surface-quenched and -unquenched cells was measured by flow cytometry. The percent internalization at each time point was calculated as: $\varepsilon = 1$ – quench MFI (T0) / unquench MFI (T0). The internalization percentage was calculated as: (1 – (unquench MFI (Tn) – quenched MFI (Tn)) / ($\varepsilon \times$ unquench MFI (Tn))) $\times$ 100%. T0 indicates the initial fluorescent signals without incubation, and Tn indicates the incubation time point groups.

Cell viability

Cells grown on 96-well white plates were treated with the indicated compounds for 144 h. Viable cells were detected using the CellTiter-Glo® Luminescent Cell Viability Assay (Promega, Cat #: G7572) following the manufacturer's instructions. Briefly, the cells treated with compounds were lysed using a 1:1 mixture of CellTiter-Glo® Reagent and culture media for 10 min. After the incubation, the luminescence was recorded by a SpectraMax M2 reader. The concentration of half maximal growth inhibitory (IC_{50}) was calculated by GraphPad Prism 6.

Western blot

Cells were lysed in Laemmli sample buffer (LSB; 60 mM Tris (pH 6.8), 2% sodium dodecylsulfate (SDS) and 10% glycerol). The proteins were separated on 4–20% SDS-PAGE followed by transferring onto a Polyvinylidene fluoride (PVDF) membrane. Target proteins on PVDF were probed with primary antibodies: anti-RPA2 pS4/S8 (Bethyl Cat# A300-245A, RRID:AB_210547), anti-RPA2 (Abcam Cat# ab2175, RRID:AB_302873), anti-γH2AX (Santa Cruz Biotechnology Cat# sc-517348, RRID:AB_2783871), anti-H2AX (Cell Signaling Technology Cat# 2595, RRID:AB_10694556), anti-Actin (Millipore Cat# MAB1501, RRID:AB_2223041), anti-P-glycoprotein (Abcam Cat# ab129450, RRID:AB_11157199), anti-BCRP (Abcam Cat#ab207732), anti-TOP1 (Sigma-Aldrich Cat# HPA019039, RRID:AB_1858187), anti-TROP2 (Abcam Cat# ab214488, RRID:AB_2811182) and anti-β-Tubulin (Arigo Cat# ARG62347, RRID:AB_2810997). After incubation overnight, the membranes were incubated with Horseradish peroxidase (HRP) conjugated goat anti-mouse (Jackson ImmunoResearch Labs Cat# 115–035-003, RRID:AB_10015289) or anti-rabbit (Jackson ImmunoResearch Labs Cat# 111–035-003, RRID:AB_2313567) antibodies to detect the target proteins. The intensity of the chemiluminescence of the bands represents the level of the proteins.

Quantitative flow cytometry

Cells were stained with AF488-conjugated mouse anti-human TROP2 antibody (clone 77,220, R&D system) or isotype control antibody, and then analyzed by BD Canto II Flow Cytometry. The number of binding sites of the anti-human TROP2 antibody on cells were calculated using Quantum™ Simply Cellular® (QSC) anti-Mouse IgG kit (Bangs Laboratories, Catalog #: 815.) according to the manufacturer's instructions. In brief, the QSC calibration microspheres coated with increasing amounts of capture antibody were labeled to saturation with the same antibody used to label cells. The mean fluorescence index (MFI) of the labeled calibration microspheres and cells were recorded and analyzed using QuickCal® analysis template (Bangs Laboratories, Lot #: 15,514.) to determine the Antibody Binding Capacity value of each cell.

Viability evaluation of spheroid cells with ADC treatment

DU-145 cells were seeded on 96-well ultra-low attachment microplate (Corning®, Level Biotechnology Inc., Taiwan) at 150 cells/well. The plates were centrifuged at 400 g for 5 min followed by culturing at 37 °C with 5% CO_2 for 4–6 days to form spheroids. After forming spheroids, cells were treated with ADC for 144 h. Viable cells were detected using the CellTiter-Glo® 3D Cell Viability Assay (Promega) following the manufacturer's instructions. Briefly, the ADC-treated cells were lysed using a 1:1 mixture of CellTiter-Glo® 3D Reagent and culture media for 30 min. The resulting solution was transferred to 96-well white plates. Luminescence was

recorded using the SpectraMax M2. The concentration of half maximal growth inhibition (IC_{50}) was calculated by using GraphPad Prism 6.

Establishment of ADC-resistant colorectal adenocarcinoma cell lines
DLD-1 colorectal adenocarcinoma cells were treated sequentially with increasing concentrations of OBI-992, SG, or Dato-DXd to induce ADC-resistant cell lines. Cells were iteratively exposed to ADCs for 3 days, followed by a recovery period of approximately 4–11 days without treatment. The treatment procedure involved stepwise increases of the concentrations of OBI-992 (100 nM to 500 nM), SG (0.3 nM to 120 nM), and Dato-DXd (50 nM to 500 nM) over a period of approximately 6 months.

Data availability
All data generated or analyzed during this study are included in this published article and its Supplementary Information files.

References

1. Khongorzul, P., Ling, C. J., Khan, F. U., Ihsan, A. U. & Zhang, J. Antibody-Drug Conjugates: A Comprehensive Review. *Mol. Cancer Res.* **18**, 3–19. https://doi.org/10.1158/1541-7786.Mcr-19-0582 (2020).
2. Marei, H. E., Cenciarelli, C. & Hasan, A. Potential of antibody-drug conjugates (ADCs) for cancer therapy. *Cancer Cell Int.* **22**, 255. https://doi.org/10.1186/s12935-022-02679-8 (2022).
3. Samantasinghar, A. et al. A comprehensive review of key factors affecting the efficacy of antibody drug conjugate. *Biomed. Pharmacother.* **161**, 114408. https://doi.org/10.1016/j.biopha.2023.114408 (2023).
4. Shen, L. et al. ADCdb: the database of antibody-drug conjugates. *Nucleic. Acids Res.* **52**, D1097–D1109. https://doi.org/10.1093/nar/gkad831 (2024).
5. Ripani, E., Sacchetti, A., Corda, D. & Alberti, S. Human Trop-2 is a tumor-associated calcium signal transducer. *Int. J. Cancer* **76**, 671–676. https://doi.org/10.1002/(sici)1097-0215(19980529)76:5%3c671::aid-ijc10%3e3.0.co;2-7 (1998).
6. Shvartsur, A. & Bonavida, B. Trop2 and its overexpression in cancers: regulation and clinical/therapeutic implications. *Genes Cancer* **6**, 84–105. https://doi.org/10.18632/genesandcancer.40 (2015).
7. Lin, H. et al. Significantly upregulated TACSTD2 and Cyclin D1 correlate with poor prognosis of invasive ductal breast cancer. *Exp Mol Pathol* **94**, 73–78. https://doi.org/10.1016/j.yexmp.2012.08.004 (2013).
8. Xu, P. et al. Prognostic role and clinical significance of trophoblast cell surface antigen 2 in various carcinomas. *Cancer Manag Res.* **9**, 821–837. https://doi.org/10.2147/cmar.S147033 (2017).
9. Zeng, P. et al. Impact of TROP2 expression on prognosis in solid tumors: A Systematic Review and Meta-analysis. *Sci. Rep.* **6**, 33658. https://doi.org/10.1038/srep33658 (2016).
10. Cubas, R., Zhang, S., Li, M., Chen, C. & Yao, Q. Trop2 expression contributes to tumor pathogenesis by activating the ERK MAPK pathway. *Mol. Cancer* **9**, 253. https://doi.org/10.1186/1476-4598-9-253 (2010).
11. Goldenberg, D. M., Stein, R. & Sharkey, R. M. The emergence of trophoblast cell-surface antigen 2 (TROP-2) as a novel cancer target. *Oncotarget* **9**, 28989–29006. https://doi.org/10.18632/oncotarget.25615 (2018).
12. Pommier, Y., Nussenzweig, A., Takeda, S. & Austin, C. Human topoisomerases and their roles in genome stability and organization. *Nat. Rev. Mol. Cell Biol.* **23**, 407–427. https://doi.org/10.1038/s41580-022-00452-3 (2022).
13. Pommier, Y., Sun, Y., Huang, S. N. & Nitiss, J. L. Roles of eukaryotic topoisomerases in transcription, replication and genomic stability. *Nat. Rev. Mol. Cell. Biol.* **17**, 703–721. https://doi.org/10.1038/nrm.2016.111 (2016).
14. Champoux, J. J. DNA topoisomerases: structure, function, and mechanism. *Annu. Rev. Biochem.* **70**, 369–413. https://doi.org/10.1146/annurev.biochem.70.1.369 (2001).
15. Pommier, Y. Drugging topoisomerases: lessons and challenges. *ACS Chem. Biol.* **8**, 82–95. https://doi.org/10.1021/cb300648v (2013).
16. Xu, Y. & Her, C. Inhibition of Topoisomerase (DNA) I (TOP1): DNA Damage Repair and Anticancer Therapy. *Biomolecules* **5**, 1652–1670. https://doi.org/10.3390/biom5031652 (2015).
17. Pommier, Y. & Marchand, C. Interfacial inhibitors: targeting macromolecular complexes. *Nat. Rev. Drug. Discov.* **11**, 25–36. https://doi.org/10.1038/nrd3404 (2011).
18. Syed, Y. Y. Sacituzumab Govitecan: First Approval. *Drugs* **80**, 1019–1025. https://doi.org/10.1007/s40265-020-01337-5 (2020).
19. Kiyotaka Yoh, Y. G. et al. A randomized, phase 3 study of datopotamab deruxtecan (Dato-DXd; DS-1062) versus docetaxel in previously treated advanced or metastatic non-small cell lung cancer (NSCLC) without actionable genomic alterations (TROPION-Lung01). *J. Clinic. Oncol.* https://doi.org/10.1200/JCO.2021.39.15_suppl.TPS9127, (2021).
20. Fang, W. et al. SKB264 (TROP2-ADC) for the treatment of patients with advanced NSCLC: Efficacy and safety data from a phase 2 study. *J. Clinic. Oncol.* **41**, suppl. https://ascopubs.org/doi/pdf/10.1200/JCO.2023.41.16_suppl.9114 (2023).
21. Abou-Alfa, G. K. et al. Randomized phase III study of exatecan and gemcitabine compared with gemcitabine alone in untreated advanced pancreatic cancer. *J. Clin. Oncol.* **24**, 4441–4447. https://doi.org/10.1200/jco.2006.07.0201 (2006).
22. Fontaine, S. D., Carreras, C. W., Reid, R. R., Ashley, G. W. & Santi, D. V. A Very Long-acting Exatecan and Its Synergism with DNA Damage Response Inhibitors. *Cancer Res. Commun.* **3**, 908–916. https://doi.org/10.1158/2767-9764.CRC-22-0517 (2023).
23. Jo, U. et al. TOP1-DNA Trapping by Exatecan and Combination Therapy with ATR Inhibitor. *Mol. Cancer Ther.* **21**, 1090–1102. https://doi.org/10.1158/1535-7163.Mct-21-1000 (2022).
24. Mitsui, I. et al. A new water-soluble camptothecin derivative, DX-8951f, exhibits potent antitumor activity against human tumors in vitro and in vivo. *Jpn. J. Cancer Res.* **86**, 776–782. https://doi.org/10.1111/j.1349-7006.1995.tb02468.x (1995).
25. Braybrooke, J. P. et al. Phase I and pharmacokinetic study of the topoisomerase I inhibitor, exatecan mesylate (DX-8951f), using a weekly 30-minute intravenous infusion, in patients with advanced solid malignancies. *Ann. Oncol.* **14**, 913–921. https://doi.org/10.1093/annonc/mdg243 (2003).
26. Li, F., Jiang, T., Li, Q. & Ling, X. Camptothecin (CPT) and its derivatives are known to target topoisomerase I (Top1) as their mechanism of action: did we miss something in CPT analogue molecular targets for treating human disease such as cancer?. *Am. J. Cancer Res.* **7**, 2350–2394 (2017).
27. Das, S. K. et al. Poly(ADP-ribose) polymers regulate DNA topoisomerase I (Top1) nuclear dynamics and camptothecin sensitivity in living cells. *Nucl. Acids Res.* **44**, 8363–8375. https://doi.org/10.1093/nar/gkw665 (2016).
28. Weng, W. et al. Antibody-Exatecan Conjugates with a Novel Self-immolative Moiety Overcome Resistance in Colon and Lung Cancer. *Cancer Discov.* **13**, 950–973. https://doi.org/10.1158/2159-8290.Cd-22-1368 (2023).
29. Ray Chaudhuri, A. & Nussenzweig, A. The multifaceted roles of PARP1 in DNA repair and chromatin remodelling. *Nat. Rev. Mol. Cell Biol.* **18**, 610–621. https://doi.org/10.1038/nrm.2017.53 (2017).

30. Malanga, M. & Althaus, F. R. Poly(ADP-ribose) reactivates stalled DNA topoisomerase I and Induces DNA strand break resealing. *J. Biol. Chem.* **279**, 5244–5248. https://doi.org/10.1074/jbc.C300437200 (2004).
31. Chowdhuri, S. P. & Das, B. B. Top1-PARP1 association and beyond: from DNA topology to break repair. *NAR* https://doi.org/10.1093/narcan/zcab003 (2021).
32. Davidson, D., Wang, Y., Aloyz, R. & Panasci, L. The PARP inhibitor ABT-888 synergizes irinotecan treatment of colon cancer cell lines. *Invest. N. Drugs* **31**, 461–468. https://doi.org/10.1007/s10637-012-9886-7 (2013).
33. Ray Chaudhuri, A. *et al.* Topoisomerase I poisoning results in PARP-mediated replication fork reversal. *Nat Struct Mol Biol* **19**, 417–423, https://doi.org/10.1038/nsmb.2258 (2012).
34. Tahara, M. et al. The use of Olaparib (AZD2281) potentiates SN-38 cytotoxicity in colon cancer cells by indirect inhibition of Rad51-mediated repair of DNA double-strand breaks. *Mol. Cancer Ther.* **13**, 1170–1180. https://doi.org/10.1158/1535-7163.Mct-13-0683 (2014).
35. Patel, A. G. et al. Enhanced killing of cancer cells by poly(ADP-ribose) polymerase inhibitors and topoisomerase I inhibitors reflects poisoning of both enzymes. *J. Biol. Chem.* **287**, 4198–4210. https://doi.org/10.1074/jbc.M111.296475 (2012).
36. Bardia, A. et al. Antibody Drug Conjugate Sacituzumab Govitecan Enables A Sequential TOP1/PARP Inhibitor Cancer Therapy Strategy in Breast Cancer Patients. *Clin. Cancer Res.* https://doi.org/10.1158/1078-0432.CCR-24-0428 (2024).
37. Li, W. F. et al. OBI-992, a Novel TROP2-Targeted Antibody-Drug Conjugate, Demonstrates Antitumor Activity in Multiple Cancer Models. *Mol. Cancer Ther.* **24**, 163–175. https://doi.org/10.1158/1535-7163.Mct-24-0588 (2025).
38. Zhao, H. et al. A Potential Mechanism for ADC-Induced Neutropenia: Role of Neutrophils in Their Own Demise. *Mol. Cancer Ther.* **16**, 1866–1876. https://doi.org/10.1158/1535-7163.Mct-17-0133 (2017).
39. Ocean, A. J. et al. Sacituzumab govitecan (IMMU-132), an anti-Trop-2-SN-38 antibody-drug conjugate for the treatment of diverse epithelial cancers: Safety and pharmacokinetics. *Cancer* **123**, 3843–3854. https://doi.org/10.1002/cncr.30789 (2017).
40. Fontaine, S. D., Reid, R., Robinson, L., Ashley, G. W. & Santi, D. V. Long-term stabilization of maleimide-thiol conjugates. *Bioconjug Chem.* **26**, 145–152. https://doi.org/10.1021/bc5005262 (2015).
41. Kopp, A. et al. Antibody-Drug Conjugate Sacituzumab Govitecan Drives Efficient Tissue Penetration and Rapid Intracellular Drug Release. *Mol. Cancer Ther.* **22**, 102–111. https://doi.org/10.1158/1535-7163.Mct-22-0375 (2023).
42. Borst, P. & Elferink, R. O. Mammalian ABC transporters in health and disease. *Annu. Rev. Biochem.* **71**, 537–592. https://doi.org/10.1146/annurev.biochem.71.102301.093055 (2002).
43. Cardillo, T. M. et al. Synthetic Lethality Exploitation by an Anti-Trop-2-SN-38 Antibody-Drug Conjugate, IMMU-132, Plus PARP Inhibitors in BRCA1/2-wild-type Triple-Negative Breast Cancer. *Clin. Cancer Res.* **23**, 3405–3415. https://doi.org/10.1158/1078-0432.Ccr-16-2401 (2017).
44. Joubert, M. K. et al. Highly aggregated antibody therapeutics can enhance the in vitro innate and late-stage T-cell immune responses. *J. Biol. Chem.* **287**, 25266–25279. https://doi.org/10.1074/jbc.M111.330902 (2012).
45. Tada, M., Aoyama, M. & Ishii-Watabe, A. Fcgamma Receptor Activation by Human Monoclonal Antibody Aggregates. *J. Pharm. Sci.* **109**, 576–583. https://doi.org/10.1016/j.xphs.2019.10.046 (2020).
46. Okajima, D. et al. Datopotamab Deruxtecan, a Novel TROP2-directed Antibody-drug Conjugate, Demonstrates Potent Antitumor Activity by Efficient Drug Delivery to Tumor Cells. *Mol. Cancer Ther.* **20**, 2329–2340. https://doi.org/10.1158/1535-7163.Mct-21-0206 (2021).
47. Sun, M. et al. Structural insights into the cis and trans assembly of human trophoblast cell surface antigen 2. *Iscience* https://doi.org/10.1016/j.isci.2021.103190 (2021).
48. Kumar, S. & Sherman, M. Y. Resistance to TOP-1 Inhibitors: Good Old Drugs Still Can Surprise Us. *Int. J. Mol. Sci.* https://doi.org/10.3390/ijms24087233 (2023).
49. Dotan, E. et al. Phase I/II Trial of Labetuzumab Govitecan (Anti-CEACAM5/SN-38 Antibody-Drug Conjugate) in Patients With Refractory or Relapsing Metastatic Colorectal Cancer. *J Clin Oncol* **35**, 3338–3346. https://doi.org/10.1200/jco.2017.73.9011 (2017).
50. Spring, L. M. et al. Sacituzumab Govitecan for Metastatic Triple-Negative Breast Cancer: Clinical Overview and Management of Potential Toxicities. *Oncologist* **26**, 827–834. https://doi.org/10.1002/onco.13878 (2021).
51. Nguyen, T. D., Bordeau, B. M. & Balthasar, J. P. Mechanisms of ADC Toxicity and Strategies to Increase ADC Tolerability. *Cancers (Basel)* https://doi.org/10.3390/cancers15030713 (2023).
52. Liao-Chan, S. et al. Quantitative assessment of antibody internalization with novel monoclonal antibodies against Alexa fluorophores. *PLoS One* https://doi.org/10.1371/journal.pone.0124708 (2015).

Acknowledgements

Author contributions

T.-Y. Chang: Conceptualization, Formal Analysis, Visualization, Investigation, and Writing – original draft. C.-J. Lin, S.-N Wen: Formal Analysis, Visualization, and Investigation. Y.-C. Wu, C.-Y. Wei, J.-Y. Hung, Y.-H. Tsao, Y.-J. Chen, Y.-C. Wu: Formal Analysis and Investigation. W.-C. Tang: Investigation and Supervision. W.-H. Lee, T.-Y. Huang, T.-M. Kuo, and W.-F. Li: Conceptualization and Supervision. M.-T. Lai: Conceptualization, Supervision, and Writing – review & editing.

Declarations

Competing interests

The authors declare no competing interests.

Additional information

Supplementary Information The online version contains supplementary material available at https://doi.org/10.1038/s41598-025-92697-z.

Correspondence and requests for materials should be addressed to M.-T.L.

Reprints and permissions information is available at www.nature.com/reprints.

Publisher's note Springer Nature remains neutral with regard to jurisdictional claims in published maps and institutional affiliations.